KIMATA, M. & SAITO, S. (1987). *Abstracts of the Annual Meeting of the Mineralogical Society of Japan, the Society of Mining Geologists of Japan and the Japanese Association of Mineralogists, Petrologists and Economic Geologists*, p. 39. (In Japanese).
KNOP, O., REID, K. I. G., SUTARNO & NAKAGAWA, Y. (1968). *Can. J. Chem.* **46**, 3463–3476.
MERWIN, L. H., SEBALD, A. & SEIFERT, F. (1989). *Phys. Chem. Miner.* **16**, 752–756.
RAAZ, F. (1930). *Anz. Akad. Wiss. Wien Math. Naturwiss. Kl.* **18**, 203.
SEIFERT, F., CZANK, M., SIMONS, B. & SCHMAHL, W. (1987). *Phys. Chem. Miner.* **14**, 26–35.
STOUT, G. H. & JENSEN, L. H. (1989). *X-ray Structure Determination*. New York: Wiley.
WARREN, B. E. (1930). *Z. Kristallogr.* **74**, 131–138.
WOLFF, P. M. DE (1974). *Acta Cryst.* A**30**, 777–785.
YAMAMOTO, A. (1982). *Acta Cryst.* A**38**, 87–92.
YAMAMOTO, A. (1984). *REMOS*82.1. A computer program for the refinement of modulated structures. National Institute for Research in Inorganic Materials, Sakura-mura, Niihari-gun, Ibaraki 305, Japan.

Acta Cryst. (1993). B**49**, 179–192

The Experimental Electron Density in Monoclinic Cobalt Sulfate Hexahydrate, $CoSO_4.6D_2O$, at 25 K*

BY THOMAS KELLERSOHN†

Anorganische Chemie I, *Universität GH Siegen, Postfach* 101240, *W*-5900 *Siegen, Germany*

ROBERT G. DELAPLANE AND IVAR OLOVSSON

Department of Inorganic Chemistry, Institute of Chemistry, Uppsala University, Box 531, *S*-751 21 *Uppsala, Sweden*

AND GARRY J. MCINTYRE

Institut Laue–Langevin, BP 156, *F*-38042 *Grenoble CEDEX* 9, *France*

(*Received* 20 *May* 1992; *accepted* 20 *August* 1992)

Abstract

The electron density in $CoSO_4.6D_2O$ has been determined at 25 K by multipole refinement against single-crystal X-ray intensity data. Hydrogen positional and displacement parameters have been taken from a refinement using single-crystal neutron data. The influence of superposition on the total deformation density has been assessed by calculating the densities separately from the deformation functions of the individual constituents of the structure. The deformation density is significantly distorted from octahedral symmetry for the two crystallographically independent Co^{2+} ions, although the water O-atom arrangement around them is close to octahedral in both cases. The individual deformation densities for the six water molecules show clear polarization effects in the oxygen lone-pair region, which correspond to the respective coordination modes, ranging from trigonal planar to tetrahedral. The results are compared with those of similar studies on both tetragonal and monoclinic $NiSO_4.6(H,D)_2O$. Crystal data: cobalt(II) sulfate hexahydrate ($-d_{12}$), $CoSO_4.6D_2O$, $M_r = 275.15$, monoclinic, $C2/c$, $a = 10.006\ (5)$, $b = 7.252\ (4)$, $c = 24.122\ (12)$ Å, $\beta = 98.96\ (4)°$, $V = 1729.0\ (9)$ Å^3, $Z = 8$, $D_x = 2.03$ g cm^{-3}; λ(Mo $K\alpha$) = 0.71073 Å, $\mu = 29.90$ cm^{-1}, $F(000) = 1080$, $T = 25$ K, $R(F) = 0.0186$ for 4676 observed unique reflections up to $[(\sin\theta)/\lambda]_{max} = 0.995$ Å^{-1} (X-ray); $R(F) = 0.0407$ for 3963 observed reflections up to $[(\sin\theta)/\lambda]_{max} = 0.910$ Å^{-1} (neutron).

1. Introduction

The *d*-electron distribution around first-row transition-metal ions has been the subject of a large number of experimental studies during the last decade. For some recent reviews, see Angermund, Claus, Goddard & Krüger (1985), Hall (1986) and Coppens (1989). Generally, such studies have to deal with many difficulties due to the higher absorption coefficients of materials containing heavier atoms and, because of the large inert cores, only a small fraction of the total scattering arises from the valence electrons. On the other hand, the contraction of the *d*-electron shell of the heavier elements of the first transition row gives somewhat stronger scattering at

* Hydrogen Bond Studies 157. Part 156: Kellersohn, Delaplane & Olovsson (1991).

† Present address: Anorganisch-Chemisches Institut der Universität Bonn, Gerhard-Domagk-Strasse 1, W-5300 Bonn, Germany.

0108-7681/93/020179-14$06.00

higher angles compared to the valence electrons of the lighter members. From this point of view, cobalt and nickel are, relatively speaking, favourable among the 3*d* elements. Copper takes a special position, since the Jahn–Teller distortion arising from its d^9 configuration frequently gives special structure types that are not related to the corresponding Co and Ni compounds and a comparative study is therefore not possible.

Owing to the increasing amount of experimental material that has become available, it now seems possible to evaluate the accuracy of a given study and to reveal trends in the electron distribution within the first transition-metal row. For the latter purpose, the metal ions in question should be studied in comparable crystalline environments. An excellent study in this spirit has been performed by Maslen & Spadaccini (1989) on the perovskite-type $KM^{II}F_3$ series. The features in their difference electron density maps (*i.e.* the charge depletion in the *M*—F bonds and the charge accumulation in the sections between them) increased consistently in height on going from Mn to Ni. However, in this structure type the environment of the metal ions has a high crystallographic symmetry, which is a disadvantage when the distortion of the *d*-electron distribution due to the actual bonding situation is to be investigated. Therefore, the Tutton's salt series $M^{I}_2M^{II}(SO_4)_2.6H_2O$ have been chosen as model compounds (Maslen, Ridout & Watson, 1988; Maslen, Watson & Moore, 1988). These studies suggest that a deviation of the *d*-electron distribution from 432 symmetry can be significant, even when the nearest-neighbour arrangement is still nearly octahedral. Therefore, the observed distortions around the metal ions have been attributed to next-nearest-neighbour interactions. This is contrary to common wisdom, which interprets chemical bonding as a short-range phenomenon. To obtain complementary data, it would be an advantage to study a series of model compounds that offer two (or more, although this occurs rarely) crystallographically independent transition-metal ions of the same kind on different crystallographic sites but in similar environments to make an internal comparison possible. For this reason, the monoclinic $M^{II}SO_4.6H_2O$-type compounds, which fulfil this criterion, are interesting candidates.

Moreover, the tetragonal form of $NiSO_4.6(H,D)_2O$ has already been the subject of extensive electron density studies both at room temperature (McIntyre, Ptasiewicz-Bak & Olovsson, 1990) and at 25 K (Ptasiewicz-Bak, Olovsson & McIntyre, 1993). In that compound, the *d*-electron distribution around the Ni ion shows only very small deviations from octahedral symmetry (if at all significant), although the site symmetry for Ni is only 2. A comparison with the monoclinic form is highly desirable and the corresponding investigations are in progress (Ptasiewicz-Bak, McIntyre & Olovsson, 1993). The electron density of monoclinic $CoSO_4.6D_2O$ is reported in the present paper. The occurrence of six crystallographically independent water molecules in environments ranging from trigonally planar to tetrahedral offers an additional possibility to check the reliability of the results, since for water molecules the expected deformation density features are now quite well established from numerous similar experimental studies (for a review, see Hermansson, 1984) as well as theoretical calculations (see, for example, Hermansson, Olovsson & Lunell, 1984; Hermansson, 1985), which can serve as a reference.

2. Experimental

Slow evaporation of a solution of previously dried (600 K for 24 h) $CoSO_4$ in 90% D_2O/10% D_2SO_4 at room temperature produced deep-red translucent hexagonal platelets or hexagonal pyramids of $CoSO_4.6D_2O$. When the acid concentration increases during evaporation, we observed that the hexahydrate crystals dissolve again and the monohydrate precipitates in microcrystalline form, together with usually very few well developed crystals of the tetrahydrate (Kellersohn, 1992). From a neutral D_2O solution, the heptahydrate can be obtained (Kellersohn, Delaplane & Olovsson, 1991).

Neutron data

The crystal used for the neutron data collection was a hexagonal plate with maximum dimensions 2.7 × 2.4 × 1.2 mm. Diffraction data were measured at the ILL on the four-circle diffractometer D19, which is equipped with a 4 × 64° position-sensitive detector. The sample temperature was maintained at 25.0 ± 0.2 K (estimated absolute inaccuracy ± 1 K) by a Displex cryo-refrigerator. Two sets of 1305 and 4025 reflections were scanned in normal-beam Weissenberg geometry at wavelengths 1.3150 and 0.9562 Å, respectively, obtained by reflection of the thermal neutron beam from the (115) and (117) planes of a Ge monochromator.

Four standard reflections measured at regular time intervals showed no significant intensity variation. The three-dimensional count distribution around each reciprocal-lattice point was corrected for background and reduced to an integrated intensity *I* by a method that minimizes the relative standard deviation, $\sigma(I)/I$ (Wilkinson, Khamis, Stansfield & McIntyre, 1988). A Lorentz correction was applied, as well as an absorption correction by Gaussian integration using the calculated attenuation coefficients, $\mu_{calc} = 0.262$ and 0.208 cm^{-1} for wavelengths 1.3150 and 0.9562 Å, respectively. The correspond-

ing minimum/maximum transmission ranges were 0.927/0.971 and 0.943/0.977.

The total data corresponded to a nearly complete set of unique reflections with $|h| \le 15$, $|k| \le 9$, $|l| \le 32$ up to $(\sin\theta)/\lambda = 0.910$ Å^{-1}, but were not merged or averaged over symmetry-related reflections because of differences due to extinction, a correction of which was attempted using an anisotropic model in the refinements. Averaging over repeatedly measured reflections gave $R_{int}(I) = 0.0203$ (for the 1.3150 Å data set) and $R_{int}(I) = 0.0469$ (0.9562 Å data).

X-ray data

For the X-ray data collection, an approximately spherical crystal (aged in solution) was used that had a mean diameter of 0.18 mm. To avoid decomposition and exchange of deuterium for hydrogen, the crystal was coated with a thin film of polystyrene. Data were collected on a Huber–Aracor four-circle diffractometer equipped with a χ circle of 400 mm and a two-stage closed-cycle helium refrigerator (Samson, Goldish & Dick, 1980). The sample temperature was held at 25.0 ± 0.5 K (long-time stability); the absolute accuracy was estimated to be better than ± 2 K. Graphite (002) monochromatized Mo $K\alpha$ radiation was used, the cell dimensions were determined by a least-squares fit to the setting angles of 30 well centred reflections in the range $20° < 2\theta < 30°$. Data collection in ω–2θ mode, step scans, $\Delta\omega = 0.010°$ with a minimum number of 70 steps, maximum measuring time 3.0 s step^{-1}. A complete sphere of reflections (four unique sets) was measured up to $2\theta = 30°$ with $|h| \le 7$, $|k| \le 5$, $|l| \le 18$; thereafter a hemisphere of reflections (two unique sets) was collected up to $2\theta_{max} = 90°$, $|h| \le 20$, $-14 \le k \le 0$, $|l| \le 48$. However, the last measured shell, $75° < 2\theta < 90°$, was somewhat incomplete due to a malfunction of the cooling system followed by decomposition of the crystal (about 600 of *ca* 3000 unique reflections are missing in this shell). A total of 14117 reflections were measured. Lorentz and polarization corrections were applied, as well as background corrections according to Lehmann & Larsen (1974). The intensities of six check reflections, measured every 3 h, decreased linearly by 12.2% during the 550 h of data collection, most probably due to a slow decay of the X-ray tube. The data were correspondingly corrected. Absorption effects were corrected spherically, with maximum/minimum transmission factors 0.719/0.714. Averaging of symmetry-related reflections gave 6001 unique reflections, $R_{int}(I) = 0.0320$.

3. Refinements

All X-ray data reduction programs and the full-matrix least-squares refinement program *DUPALS* have been described by Lundgren (1982). The atomic positions reported by Elerman (1988) were used as starting values. The atomic numbering scheme and choice of asymmetric unit as given by Angel & Finger (1988) for monoclinic $NiSO_4.6H_2O$ was employed here and in the parallel electron density investigation on monoclinic $NiSO_4.6H_2O$ that is in progress to facilitate a comparison. Refinements were considered converged when $|\Delta/\sigma|_{max} < 0.01$. Final atomic coordinates and displacement parameters are given in Table 1.*

Neutron data

The scattering lengths used were 2.50, 2.847, 5.803 and 6.671 fm for Co, S, O and D, respectively (Sears, 1986). Due to the quite large crystal size and its good perfection, extinction was found to be a problem. Several extinction models, isotropic as well as anisotropic, within the Becker & Coppens (1974, 1975) formalism were tried; the best agreement was found for an anisotropic type-I model with a Lorentzian mosaic-spread distribution and the anisotropy of the mosaic spread described according to Thornley & Nelmes (1974). The quantity minimized was $\sum w(|F_o| - |F_c|)^2$, where $w^{-1} = \sigma^2_{count}|F_o| + k^2|F_o|^2$. The constant k was determined empirically from weighting analyses for different values of k; the most uniform error distribution as judged from a δR plot according to Abrahams & Keve (1971) was found for $k = 0.05$, which also corresponds closely to the value determined from the temporal variation of the standard reflections. 22 reflections suffering more than 50% from extinction were omitted in the final refinements. Atomic positional parameters were found to be quite insensitive to the extinction model used, but the displacement parameters showed some dependence. However, even in the 'best' model, the anisotropic displacement parameters of the two Co atoms could not be refined to physically reasonable values, probably due to both their very small absolute values and the small scattering length of Co relative to the other atoms, which makes it a 'light' atom in a neutron diffraction experiment. Therefore both Co atoms were refined with only isotropic displacement parameters, a constraint that we consider justified by the analysis of the X-ray data, where the anisotropic Co displacement parameters refined very close to isotropic. The residual dis-

* Tables giving the results of the conventional X-ray refinement, anisotropic extinction parameters, refined deformation density coefficients and observed and calculated structure factors as well as the final difference Fourier maps have been deposited with the British Library Document Supply Centre as Supplementary Publication No. SUP 55525 (77 pp.). Copies may be obtained through The Technical Editor, International Union of Crystallography, 5 Abbey Square, Chester CH1 2HU, England. [CIF reference: AB0287]

Table 1. *Fractional atomic coordinates and anisotropic displacement parameters* U_{ij} (10^{-2} Å^2) *for* $CoSO_4.6D_2O$ *at* 25 K

E.s.d.'s are given in parentheses. First row: neutron data; second row, when given: X-ray data from multipole refinement. Asterisks indicate isotropically refined atoms.

	x	y	z	U_{11}/U_{iso}	U_{22}	U_{33}	U_{12}	U_{13}	U_{23}
Co(1)	0.0	0.0	0.0	0.21 (6)*					
	0.0	0.0	0.0	0.420 (8)	0.448 (7)	0.429 (9)	0.041 (5)	−0.012 (5)	−0.064 (5)
Co(2)	0.5	0.44369 (46)	0.25	0.39 (7)*					
	0.5	0.44553 (3)	0.25	0.390 (8)	0.379 (7)	0.362 (9)	0.0	0.019 (5)	0.0
S	0.87017 (18)	0.45137 (28)	0.12286 (12)	0.32 (8)	0.29 (7)	0.39 (9)	−0.06 (6)	−0.11 (5)	0.03 (5)
	0.87070 (3)	0.45103 (4)	0.12259 (1)	0.439 (10)	0.423 (9)	0.423 (9)	0.011 (6)	0.011 (7)	0.001 (6)
O(1)	0.77630 (9)	0.59772 (15)	0.13495 (6)	0.524 (27)	0.498 (26)	0.688 (31)	−0.017 (23)	0.099 (22)	0.061 (24)
	0.77585 (8)	0.59796 (12)	0.13474 (3)	0.636 (23)	0.676 (21)	0.710 (23)	0.205 (18)	0.147 (18)	−0.061 (18)
O(2)	0.98788 (10)	0.44359 (14)	0.16787 (6)	0.778 (31)	0.560 (27)	0.813 (33)	0.071 (21)	−0.380 (23)	0.003 (22)
	0.98794 (9)	0.44382 (12)	0.16789 (4)	0.790 (25)	0.723 (23)	0.851 (26)	0.060 (18)	−0.418 (20)	−0.001 (18)
O(3)	0.91617 (10)	0.49391 (14)	0.06817 (6)	0.828 (29)	0.475 (30)	0.583 (28)	0.098 (22)	0.166 (23)	0.165 (22)
	0.91630 (9)	0.49481 (12)	0.06806 (4)	0.816 (23)	0.752 (21)	0.636 (23)	−0.020 (19)	0.305 (18)	0.061 (19)
O(4)	0.79976 (9)	0.27041 (13)	0.11727 (6)	0.613 (27)	0.228 (29)	0.749 (27)	−0.308 (23)	0.025 (22)	0.100 (23)
	0.80017 (9)	0.27015 (11)	0.11722 (4)	0.747 (23)	0.520 (21)	0.699 (23)	−0.149 (17)	0.043 (18)	0.001 (17)
O(5)	0.09343 (11)	0.22765 (15)	0.04403 (6)	0.806 (27)	0.725 (25)	0.800 (26)	−0.009 (20)	−0.016 (21)	−0.234 (22)
	0.09384 (6)	0.22752 (9)	0.04390 (3)	0.754 (22)	0.744 (20)	0.759 (23)	0.098 (17)	−0.056 (17)	−0.169 (17)
O(6)	−0.03150 (11)	0.16170 (16)	−0.07201 (7)	0.730 (28)	0.786 (27)	0.808 (28)	−0.133 (22)	−0.099 (22)	0.115 (23)
	−0.03096 (6)	0.16223 (12)	−0.07174 (3)	0.783 (23)	0.888 (22)	0.897 (23)	−0.186 (17)	−0.183 (18)	0.224 (18)
O(7)	0.19057 (10)	−0.05854 (18)	−0.01971 (7)	0.524 (28)	1.425 (32)	1.135 (30)	0.165 (24)	−0.085 (23)	−0.770 (28)
	0.19095 (9)	−0.05919 (10)	−0.01993 (3)	0.652 (23)	1.658 (28)	1.079 (26)	0.149 (19)	0.032 (18)	−0.706 (23)
O(8)	0.38094 (10)	0.65075 (16)	0.28179 (6)	0.581 (27)	0.389 (26)	0.713 (27)	−0.083 (23)	−0.053 (23)	−0.001 (22)
	0.38122 (5)	0.65121 (8)	0.28160 (3)	0.714 (22)	0.651 (19)	0.693 (23)	−0.031 (17)	0.203 (17)	−0.117 (16)
O(9)	0.38306 (11)	0.24789 (16)	0.28288 (7)	0.577 (26)	0.842 (24)	0.899 (29)	−0.079 (22)	0.285 (24)	0.204 (23)
	0.38277 (6)	0.24783 (10)	0.28277 (2)	0.662 (22)	0.712 (21)	0.857 (23)	−0.085 (16)	0.043 (18)	0.215 (17)
O(10)	0.64801 (10)	0.44770 (19)	0.32100 (7)	0.849 (29)	0.672 (27)	0.620 (27)	0.081 (23)	−0.240 (25)	0.075 (23)
	0.64769 (6)	0.44793 (8)	0.32104 (4)	0.927 (25)	0.679 (22)	0.644 (23)	−0.027 (16)	−0.104 (17)	0.008 (16)
D(51)	0.15861 (12)	0.19610 (20)	0.07707 (7)	1.555 (52)	1.947 (62)	1.648 (86)	0.121 (48)	−0.403 (57)	−0.267 (74)
D(52)	0.03565 (11)	0.32626 (16)	0.05414 (7)	1.713 (51)	0.987 (51)	1.924 (89)	0.349 (47)	−0.025 (56)	−0.180 (67)
D(61)	0.01478 (11)	0.28227 (17)	−0.06807 (7)	1.547 (51)	1.601 (62)	1.884 (92)	−0.477 (47)	0.041 (56)	0.123 (71)
D(62)	−0.12062 (11)	0.18370 (18)	−0.09256 (8)	1.300 (54)	2.008 (60)	1.913 (89)	−0.284 (48)	−0.254 (54)	0.273 (74)
D(71)	0.20489 (12)	−0.14019 (20)	−0.04961 (8)	1.790 (52)	1.846 (63)	1.677 (86)	0.117 (48)	0.405 (56)	−0.518 (79)
D(72)	0.27469 (12)	−0.02754 (20)	0.00323 (8)	1.217 (55)	3.003 (70)	1.985 (92)	−0.090 (52)	−0.043 (59)	−0.573 (79)
D(81)	0.33177 (11)	0.60474 (18)	0.31047 (7)	1.522 (47)	1.732 (58)	1.312 (81)	−0.084 (44)	0.678 (55)	0.451 (69)
D(82)	0.43071 (12)	0.75742 (16)	0.29918 (8)	1.619 (48)	1.444 (60)	1.711 (86)	−0.255 (47)	0.222 (54)	−0.441 (68)
D(91)	0.42394 (12)	0.13682 (17)	0.30024 (8)	1.728 (52)	1.207 (58)	2.212 (95)	0.206 (47)	0.203 (59)	0.633 (72)
D(92)	0.29136 (11)	0.21969 (18)	0.26559 (8)	0.889 (50)	2.328 (64)	2.448 (98)	−0.346 (45)	−0.351 (54)	0.187 (76)
D(101)	0.66380 (12)	0.33689 (18)	0.34343 (7)	2.363 (54)	1.131 (63)	1.881 (92)	−0.087 (51)	−0.297 (60)	0.573 (73)
D(102)	0.66110 (12)	0.55549 (19)	0.34511 (8)	2.146 (56)	1.337 (63)	1.691 (92)	0.000 (48)	−0.268 (61)	−0.401 (75)

agreement between neutron (isotropic) and X-ray (equivalent isotropic) displacement parameters is larger for Co(1) than for Co(2).

The 219 variable parameters included a scale factor, six anisotropic extinction parameters, the positional and anisotropic displacement parameters (isotropic for Co) of all atoms and an occupancy factor assumed to be common to all D atoms. Its refinement converged at 0.908 (3), corresponding to an effective 94.1 (3)% H to D exchange. Final $R(F) = 0.0407$, $wR(F) = 0.0673$, $S = 1.13$ for 3963 observed reflections [$I > 3\sigma(I)$]. The δR plot had a slope of 0.99, y intercept −0.08 and 33 reflections with $|\Delta/\sigma| > 4.0$. The somewhat high R and wR values reflect the high limit in $(\sin\theta)/\lambda$ and the poor statistics in the high-angle reflections. The refinement is nevertheless considered to be satisfactory since the goodness-of-fit as well as the slope of the δR plot are both close to unity. Maximum and minimum values in a final difference Fourier synthesis were less than 0.01 times the corresponding peak heights in an F_o synthesis.

X-ray data

Only the 4677 reflections with $I > 3\sigma(I)$ were used. Two sets of refinements were performed: (*a*) a conventional refinement with spherical atomic scattering factors and (*b*) deformation refinements where the aspherical valence-electron distribution was fitted to multipole deformation functions. In both sets of refinements, the neutral-atom relativistic Hartree–Fock scattering factors for Co, S and O were those of Doyle & Turner (1968), while for H (D) the non-relativistic Hartree–Fock scattering factor of Cromer & Mann (1968) was used. Anomalous-dispersion contributions were taken from Cromer & Liberman (1970). The quantity minimized was $\sum w[|F_o|^2 - |F_c|^2]^2$, where $w^{-1} = \sigma^2_{count}|F_o|^2 + k^2|F_o|^4$. The constant k was determined empirically from weighting analyses for different values of k; the most uniform error distribution was found for $k = 0.030$.

(*a*) *Conventional refinement.* The refined parameters were a scale factor, an isotropic extinction parameter [type I, Lorentzian mosaic spread, final value 0.9 (3) × 10^3], positional and anisotropic dis-

Table 2. *Selected bond distances* (Å) *and angles* (°) *based on the neutron data for* $CoSO_4.6D_2O$ *at* 25 K

E.s.d.'s are given in parentheses.

Co coordination			
Co(1)—O(5)	2 × 2.102 (1)	Co(2)—O(8)	2 × 2.132 (3)
Co(1)—O(6)	2 × 2.079 (1)	Co(2)—O(9)	2 × 2.075 (3)
Co(1)—O(7)	2 × 2.080 (1)	Co(2)—O(10)	2 × 2.083 (2)
Average	2.087 (12)		2.097 (28)
O(5)—Co(1)—O(6)	88.7 (1)	O(8)—Co(2)—O(8^{ii})	90.5 (1)
O(5)—Co(1)—O(6^{i})	91.3 (1)	O(8)—Co(2)—O(9)	88.0 (1)
O(5)—Co(1)—O(7)	85.7 (1)	O(8)—Co(2)—O(10)	93.4 (1)
O(5)—Co(1)—O(7^{i})	94.3 (1)	O(8)—Co(2)—O(10^{ii})	85.4 (1)
O(6)—Co(1)—O(7)	87.1 (1)	O(9)—Co(2)—O(9^{ii})	93.6 (2)
O(6)—Co(1)—O(7^{i})	92.9 (1)	O(9)—Co(2)—O(10)	93.8 (1)
O(5)—Co(1)—O(5^{i})	180.0	O(9)—Co(2)—O(10^{ii})	87.3 (1)
O(6)—Co(1)—O(6^{i})	180.0	O(8)—Co(2)—O(9^{ii})	178.2 (1)
O(7)—Co(1)—O(7^{i})	180.0	O(10)—Co(2)—O(10^{ii})	178.4 (2)
Sulfate ion			
S—O(1)	1.476 (2)	O(1)—S—O(2)	110.0 (2)
S—O(2)	1.473 (3)	O(1)—S—O(3)	108.6 (2)
S—O(3)	1.495 (3)	O(1)—S—O(4)	110.2 (1)
S—O(4)	1.486 (2)	O(2)—S—O(3)	109.7 (1)
		O(2)—S—O(4)	110.3 (2)
		O(3)—S—O(4)	108.0 (2)
Average	1.483 (10)		109.5 (9)

Water molecules and hydrogen bonds

O—D···O	O—D	D—O—D	D···O	O···O	O—D···O	Co—O—D
O(5)—D(51)···O(1^{iii})	0.975 (2)	108.4 (2)	1.826 (2)	2.792 (6)	170.5 (2)	114.6 (1)
O(5)—D(52)···O(3^{iv})	0.974 (2)	–	1.774 (2)	2.745 (2)	174.0 (1)	117.9 (1)
O(6)—D(61)···O(3^{v})	0.987 (2)	106.6 (2)	1.764 (2)	2.747 (2)	173.1 (2)	114.3 (2)
O(6)—D(62)···O(4^{vi})	0.964 (2)	–	1.829 (2)	2.780 (2)	168.2 (2)	122.1 (1)
O(7)—D(71)···O(4^{vii})	0.959 (2)	110.9 (2)	1.880 (2)	2.825 (2)	167.1 (2)	123.1 (1)
O(7)—D(72)···O(3^{iii})	0.961 (2)	–	1.947 (2)	2.871 (2)	161.0 (2)	125.0 (2)
O(8)—D(81)···O(1^{ii})	0.968 (2)	104.3 (2)	1.830 (2)	2.764 (2)	161.2 (1)	112.9 (1)
O(8)—D(82)···O(2^{viii})	0.978 (2)	–	1.708 (2)	2.685 (2)	177.0 (2)	115.8 (1)
O(9)—D(91)···O(2^{ix})	0.968 (2)	108.6 (2)	1.767 (2)	2.733 (2)	175.1 (1)	120.6 (1)
O(9)—D(92)···O(8^{x})	0.969 (2)	–	1.979 (2)	2.937 (2)	169.6 (2)	122.2 (2)
O(10)—D(101)···O(1^{ix})	0.968 (2)	109.8 (2)	1.882 (2)	2.810 (2)	159.6 (2)	118.8 (2)
O(10)—D(102)···O(4^{viii})	0.971 (2)	–	1.815 (2)	2.779 (2)	171.6 (2)	121.1 (2)

Symmetry operations: (i) $-x, -y, -z$; (ii) $1-x, y, \frac{1}{2}-z$; (iii) $-\frac{1}{2}+x, -\frac{1}{2}+y, z$; (iv) $-1+x, y, z$; (v) $1-x, 1-y, -z$; (vi) $\frac{1}{2}-x, \frac{1}{2}-y, -z$; (vii) $1-x, -y, -z$; (viii) $\frac{3}{2}-x, \frac{1}{2}+y, \frac{1}{2}-z$; (ix) $\frac{3}{2}-x, -\frac{1}{2}+y, \frac{1}{2}-z$; (x) $\frac{1}{2}-x, -\frac{1}{2}+y, \frac{1}{2}-z$; (xi) $\frac{1}{2}-x, \frac{1}{2}+y, \frac{1}{2}-z$.

placement parameters for Co, S and O. The D positional and displacement parameters were taken from the neutron data without modifications, although the O displacement parameters differed between X-ray and neutron data. However, these differences do not exceed three combined e.s.d.'s and no clear trend could be established. Final $R(F) = 0.0252$, $R(F^2) = 0.0380$, $wR(F^2) = 0.0791$, $S = 1.76$ for 4676 observed unique reflections with $I > 3.0\sigma(I)$ and 112 parameters. A δR plot had a slope of 0.76, y intercept -0.12 and 103 reflections with $|\Delta/\sigma| > 4.0$. These values as well as final difference Fourier maps indicated that an improvement could be expected from a more sophisticated model and they are to be compared with the results of the deformation refinements. The atomic coordinates and displacement parameters from this refinement have been deposited.*

(*b*) *Deformation refinements.* To minimize the effects of experimental noise, modelling of the electron deformation density by multipole fitting is to be preferred to $X-X_{\text{high-order}}$ or $X-N$ Fourier syntheses, even when the phase-angle error is not the major problem that it is in the case of noncentrosymmetric space groups. A comprehensive discussion of this point is given by McIntyre, Ptasiewicz-Bak & Olovsson (1990). We employed the multipole-deformation functions proposed by Hirshfeld (1971) with modifications by Harel & Hirshfeld (1975) and Hirshfeld (1977). The spherical charge density at each atomic site is modified by an expansion of up to 35 terms with the general form

$$\rho_n(r,\theta_k) = N_n r^n \exp(-\gamma r^2)\cos^n\theta_k$$

centred on the site, where r and θ_k are polar coordinates in the kth of a chosen set of axes, n and k are integers [$n = 0, 1, 2, 3, 4$; $k = 1, \ldots, (n+1)(n+2)/2$], and N_n are normalization factors. The scattering factor for each atom is then

$$f_i = f_{\text{spher},i} + \sum_i C_i \varphi_i,$$

where φ_i are the Fourier transforms of the expansion of the deformation density. The (population) parameters C_i are refinable.

* See deposition footnote.

A series of deformation refinements was performed where initially imposed symmetry constraints on the Co and S atoms were successively relaxed and the level of n increased. The significance of each increase of sophistication was checked by inspection of the goodness-of-fit and the δR plot. It was observed that during these series the δR plots changed their shape drastically from sigmoidal to closely linear, which is a very good indicator of the increasing reliability of the model. Strong correlation effects prohibited the simultaneous refinement of the γ parameters, which govern the breadth of the radial functions, together with the other deformation parameters. Therefore, their values were chosen based on our experience from previous studies. However, modification of the values within reasonable limits had very little effect on the total deformation density maps.

In the final set, the following parameters were refined:

Co(1): $n \le 4$, site symmetry $\bar{1}$, $\gamma = 3.5$; β_{ij} and 22 deformation parameters;

Co(2): $n \le 4$, site symmetry 2, $\gamma = 3.5$; y, β_{ij} and 19 deformation parameters;

S: $n \le 4$, no symmetry restrictions, $\gamma = 2.5$; x, y, z, β_{ij} and 35 deformation parameters;

$O(SO_4^{2-})$: $n \le 3$, no symmetry restrictions, $\gamma = 3.5$; x, y, z, β_{ij} and 20 deformation parameters, all sulfate O atoms treated independently;

$O(D_2O)$: $n \le 3$, $mm2$ symmetry imposed, $\gamma = 3.5$; x, y, z, β_{ij} and eight deformation parameters, all water O atoms treated independently;

D: $n \le 2$, cylindrical symmetry imposed, $\gamma = 4.0$; x, y, z, β_{ij} fixed to neutron values; five deformation parameters, all D atoms assumed to be equivalent;

and additionally the scale factor and an isotropic extinction parameter [final value $0.4\ (2) \times 10^3$] as in the conventional refinements. This set of parameters corresponds closely to model VI of McIntyre, Ptasiewicz-Bak & Olovsson (1990). The deformation density of the water O atoms was allowed to deviate from $mm2$ symmetry in the present study but, as observed in an earlier study, this did not improve the fit. Final $R(F) = 0.0186$, $R(F^2) = 0.0247$, $wR(F^2) = 0.0503$, $S = 1.14$ for the 4676 observed unique reflections and 320 parameters. The shape of the δR plot was close to linear with a slope of 0.98, y intercept -0.06 and 31 reflections with $|\Delta/\sigma| > 4.0$.

4. Results and discussion

The final coordinates of the heavy atoms from the neutron and X-ray refinements agree within three combined e.s.d.'s. The displacement parameters of S and O show satisfactory agreement; possible reasons for the disagreement for Co have already been discussed.

Structural aspects

Selected bond lengths and angles derived from the present low-temperature neutron data are listed in Table 2. A general description of the structure has been given by Zalkin, Ruben & Templeton (1962).

Co(1) is located on the 4(*a*) position, site symmetry $\bar{1}$, whereas Co(2) occupies the 4(*e*) position with symmetry 2. Both are surrounded octahedrally by six water O atoms as shown in Fig. 1. The maximum differences in the Co—O bond lengths are 0.023 (2) Å for Co(1) and 0.057 (5) Å for Co(2); the largest deviations in the O—Co—O angles are 7.2 (1) and 8.4 (2)°, respectively, for directly neighbouring O

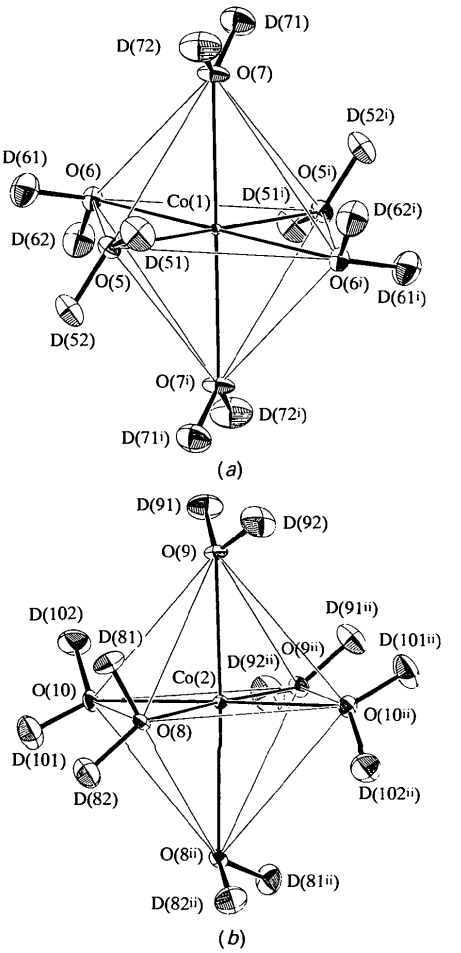

Fig. 1. Environment of (*a*) Co(1) and (*b*) Co(2). The vibrational ellipsoids (Johnson, 1976) are scaled to enclose 50% probability. Anisotropic displacement parameters are taken from the X-ray multipole refinement for Co and O and from the neutron data for D.

atoms. The distortion of the octahedron around Co(2) is therefore somewhat more pronounced. A comparison of the variation in the O—D···O angles and the angles made by Co^{2+} to the principal water planes shows that the formation of directed hydrogen bonds is a structure-determining principle and the distortion of the $[Co(D_2O)_6]^{2+}$ octahedra a secondary result. Additional complications such as disorder or structural instabilities may occur when, due to the crystal packing, hydrogen bonds of optimum strength cannot be formed for all water molecules simultaneously. This is not the case here, but it occurs, for example, in the heptahydrate (Kellersohn, Delaplane & Olovsson, 1991).

The six crystallographically independent water molecules show quite different lone-pair coordination, ranging from closely trigonally planar [O(7)], a one-sided tetrahedral [O(5), O(6), O(9), O(10)] to a complete tetrahedral environment [O(8)]; the last case involves the only water–water hydrogen bond. A quantitative picture is presented in Table 3, where the respective coordination angles as defined in Fig. 2 are listed. The intramolecular D—O—D angle is largest for the trigonally coordinated water molecule; the O—D bond lengths increase with decreasing hydrogen-bond length (D···O). These findings correspond well to the statistical analyses presented by Chiari & Ferraris (1982); see also Olovsson & Jönsson (1976). The hydrogen-bond lengths are in the range 1.708 (2) to 1.947 (2) Å for sulfate oxygen acceptors, which indicates a considerable variation in hydrogen-bond strengths. Characteristic differences of the individual water molecules can be visualized in terms of their lone-pair coordination. Thus, the trigonally coordinated $D_2O(7)$ exhibits the greatest mean D···O bond length (1.914 Å), whereas for the sole water molecule with a complete tetrahedral coordination sphere (which causes the strongest synergetic effect), $D_2O(8)$, this value is much smaller, namely 1.769 Å. The mean values for the remaining water molecules range from 1.797 to 1.870 Å. The last value should perhaps be excluded from this comparison, since it involves the only hydrogen bond with D_2O and not SO_4^{2-} as the acceptor, which is clearly the longest and weakest. Nevertheless, from solely geometric information a consistent picture of the interaction strengths emerges quite clearly.

Deformation electron densities

The Co^{2+} *ions.* The free Co^{2+} ion has a d^7 electron configuration. A Co^{2+} ion in a weak ligand field (as with water ligands in the present case) is expected to have a $d_\varepsilon^5 d_\gamma^2$ configuration. Therefore, the *d*-electron distribution should show electron depletion along the Co—O bonds and electron excess between them as a result of exchange when electron-rich ligands (such as water O atoms) come close to the *d* subshell.

Table 3. *The lone-pair coordination of the water molecules*

Angles (°) are defined according to Fig. 2. See Table 2 for symmetry operations.

Water O atom	α	β	γ	Coordinated by
O(5)	139.1 (2)	40.8 (2)	−2.8 (3)	Co(1)
O(6)	141.9 (3)	37.6 (3)	−8.1 (3)	Co(1)
O(7)	171.2 (2)	8.7 (4)	−6.6 (3)	Co(1)
O(8)	132.2 (2)	47.8 (2)	1.9 (2)	Co(2)
	−108.8 (2)	−34.2 (3)	22.2 (3)	D(92^{xi})
O(9)	153.1 (3)	26.8 (3)	−1.8 (4)	Co(2)
O(10)	150.1 (2)	29.8 (3)	−2.2 (4)	Co(2)

Furthermore, it should be symmetrical, provided that the coordination octahedra are symmetrical and that the corresponding water molecules are bound in a similar way. However, we have already noted that this is not the case.

The model deformation density maps (Fig. 3) show positive peak heights (electron excess), which are attributed to the d_ε orbitals and are in the range 0.30–0.40 e $Å^{-3}$. The negative areas are of more complex appearance and show a continuous decrease of charge density from the outer regions into the core so that a classification in terms of peak heights would give a misleading impression. Altogether, there is a significant deviation of the *d*-electron distribution from octahedral symmetry for both Co(1) and, even more pronounced, for Co(2).

These deviations do not result from superposition effects, which becomes clear from a comparison of the total maps (unprimed) with those maps where only the deformation functions centred on Co are displayed (primed). On the other hand, superposition of negative density from Co with positive density from the water O atoms does give a distorted picture in the total maps in regions close to the oxygen lone pairs (see below). A comprehensive argument in favour of the 'deconvoluted' maps has been given by Olovsson, Ptasiewicz-Bak & McIntyre (1993); see also McIntyre, Ptasiewicz-Bak & Olovsson (1990).

It has been pointed out (Mensching, von Niessen, Valtazanos, Ruedenberg & Schwarz, 1989) that for high-spin complexes the 'standard' *d* atomic orbitals maintain their orientation and shape only in exactly

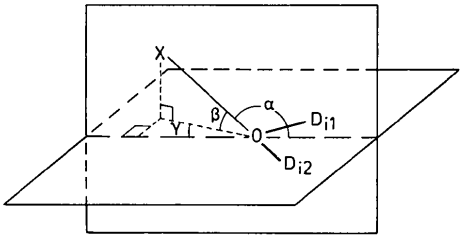

Fig. 2. The lone-pair coordination of the water molecules: definition of angles (see Table 3).

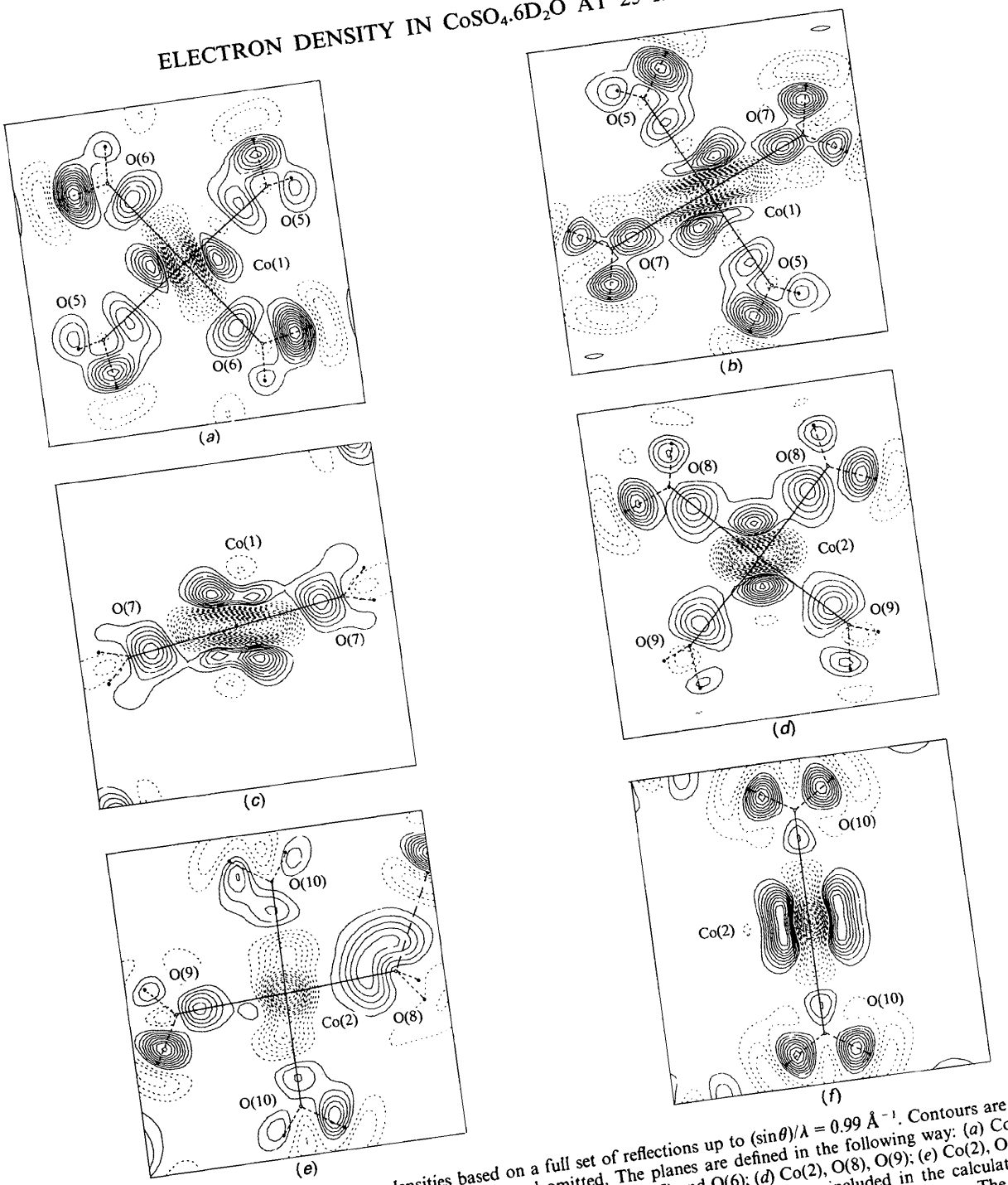

Fig. 3. $Co(D_2O)_6$ static model deformation densities based on a full set of reflections up to $(\sin\theta)/\lambda = 0.99$ Å^{-1}. Contours are drawn at intervals of 0.05 e Å^{-3}, negative contours dashed, zero level omitted. The planes are defined in the following way: (*a*) Co(1), O(5), O(6); (*b*) Co(1), O(5), O(7); (*c*) Co(1), O(7) and the inner bisector between O(5) and O(6); (*d*) Co(2), O(8), O(9); (*e*) Co(2), O(8), O(10); (*f*) Co(2), O(10) and the inner bisector between the two O(8). All deformation functions were included in the calculation of the unprimed maps, whereas the primed maps [(*a'*)–(*f'*)] display solely the deformation functions centred on the Co atoms. The scale given in (*a'*) applies to all parts of the figure. Solid lines connect atoms within the displayed plane, further connections for orientation purposes are drawn as broken lines. The long-dashed line in (*e*) and (*e'*) represents the hydrogen bond between O(8) and D(92). The labels for the D atoms have been omitted, likewise the symmetry codes.

octahedral surroundings. If the transition-metal ion in question is on a lower symmetry site, the orientation and shape as well as the populations have to be optimized. The degree of radial and angular deformation can be high especially for *d*-type atomic orbitals.

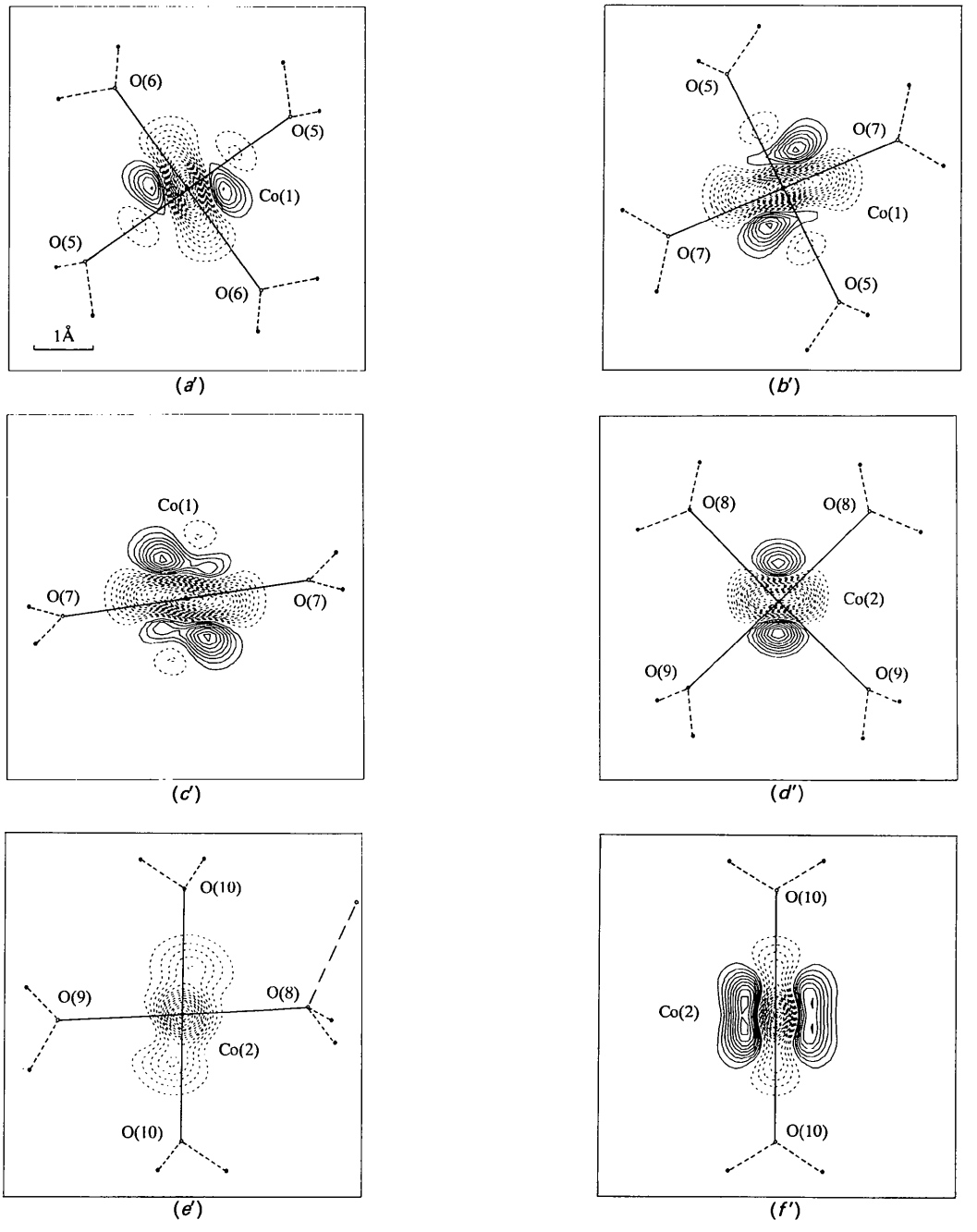

Fig. 3 (*cont.*)

The question is, to what extent can these findings be related to structural features? Coppens (1989) has summarized that in the case of a geometrically disturbed environment of a transition-metal ion, excessive *d*-electron density tends to accumulate in sterically less crowded regions, that is, within the larger *L*—*M*—*L* angles. However, it is questionable whether this reasoning applies to the present case. The maximum variation of the O—Co—O angles is 10%. A closer inspection of the maps reveals that the above statement is valid for Co(1) to a reasonable extent, but not for Co(2). This has to be compared to the results for tetragonal $NiSO_4.6(H,D)_2O$, both at room temperature and at 25 K, where the geometrical deviations within the $[Ni(D_2O)_6]^{2+}$ octahedron (also with site symmetry 2 for Ni^{2+}) are of similar magnitude to the present deviations, but the *d*-electron distribution is much more regular. On the

other hand, the $d_\varepsilon^5 d_\gamma^2$ configuration of Co^{2+} allows some redistribution of charge density within the d_ε orbitals as opposed to the $d_\varepsilon^6 d_\gamma^2$ configuration of Ni^{2+}, so that exchange and deformation interactions are probably more effective in the present case.

The suggestion that the features observed in the model density maps are real and not artefacts arising from experimental shortcomings is supported when the water maps (see below) as well as the corresponding results for the Tuttons' salt series are compared to our present study. For example, Maslen, Ridout & Watson (1988) have observed similar asymmetry features around Ni^{2+} and attributed them to next-nearest-neighbour interactions, particularly to the electrostatic field of the M^I cations close to the $[M^{II}(H_2O)_6]^{2+}$ octahedra. Although the situation is somewhat different for the $M^{II}SO_4.6H_2O$ structure type, we investigated the electrostatic field of the whole lattice in a more quantitative way by calculating the Madelung potential around the Co^{2+} sites. A local version of the program by Ross & Wahlgren (Almlöf, Roos, Wahlgren & Johansen, 1972) was employed for this purpose. In a first series, the formal charges of all atoms were used to evaluate geometric influences separately from electron redistribution effects. The potential field constructed in this way is quite symmetric in all sections around the Co^{2+} ions; an example is depicted in Fig. 4(*a*). We note, however, that the repulsive potential is less pronounced within the larger O—Co—O angles in agreement with Coppens' statement. In a second calculation, the charges derived from the multipole refinement were assigned. This procedure yielded even flatter maps, with regions suitable for *d*-electron accumulation around Co^{2+} less pronounced than before; see Fig 4(*b*). It can thus be concluded that, if next-nearest-neighbour interactions are mainly electrostatic in nature, the observed distortions of the electron density are very sensitive to changes in the electric potential field. However, because the atomic charges derived from the Hirshfeld multipole populations are quite strongly dependent on the integration method used, we do not consider the derived absolute values of the Madelung potentials to be too reliable. In contrast, the shape of the potential field should be less sensitive to these errors.

From a polarized neutron diffraction study of $[Co^{III}(NH_3)_5(H_2O)][Cr^{III}(CN)_6]$, Figgis, Kucharski & Vrtis (1991) obtained evidence that spin transfer *via* hydrogen bonds can be a further mechanism for intermolecular electronic interactions. If this applies also to the present case, it might contribute to the considerably larger asymmetry in charge density for Co(2), since the $[Co(2)(D_2O)_6]^{2+}$ entities are directly connected *via* the O(9)—D(91)···O(8) hydrogen bonds, compared to $[Co(1)(D_2O)_6]^{2+}$, which are not. However, no final interpretation of this point can be given at that moment, and further experimental evidence, also from investigations of the isostructural nickel and magnesium compounds, is therefore highly desirable.

The water molecules and the hydrogen bonds. Model maps of the electron density distribution in the DOD planes of the water molecules are shown in Fig. 5; sections normal to these planes are displayed in Fig. 6. In all cases, only the deformation functions centred on O and D are plotted (see also above). To illustrate that the superposition effect gives a distorted appearance of the deformation density in the oxygen lone-pair region, two total maps corresponding to Figs. 6(*b*) and 6(*c*) are depicted in Fig. 7. They represent cases of a one-sided tetrahedral and a trigonal coordination. The total maps in the DOD planes (not shown) are less distorted by superposition effects, with the exception of O(7).

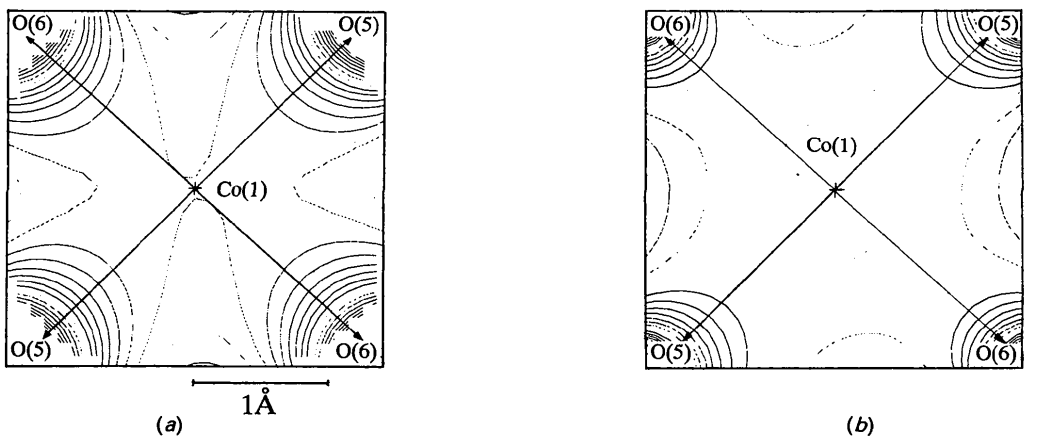

Fig. 4. Plots of the Madelung potential of the whole crystal in the plane O(5)—Co(1)—O(6). Contour lines are drawn in steps of 0.02 e $Å^{-3}$, dotted lines < −0.63 e $Å^{-3}$, full lines > −0.63 e $Å^{-3}$; (*a*) calculated on the basis of formal charges, (*b*) on the basis of charges derived from the multipole refinement.

The maps for the six different water molecules show a remarkable overall consistency even in the presence of such a strong scatterer as Co. The peak heights are in the range 0.40–0.55 e $Å^{-3}$ for O—D bonds, 0.15–0.30 e $Å^{-3}$ in the lone-pair region and uniformly -0.15 e $Å^{-3}$ close to the D atoms in the hydrogen bonds. The sequence of hydrogen-bond strengths is thus not clearly reproduced from the deformation densities. Since electrostatic interactions are the main contribution to hydrogen-bond strength this is not too surprising.

In contrast, the shape of the lone-pair peaks can be correlated quite closely with the coordination geometry, as has similarly been observed for tetragonal $NiSO_4.6(H,D)_2O$ (McIntyre, Ptasiewicz-Bak & Olovsson, 1990; Ptasiewicz-Bak, Olovsson &

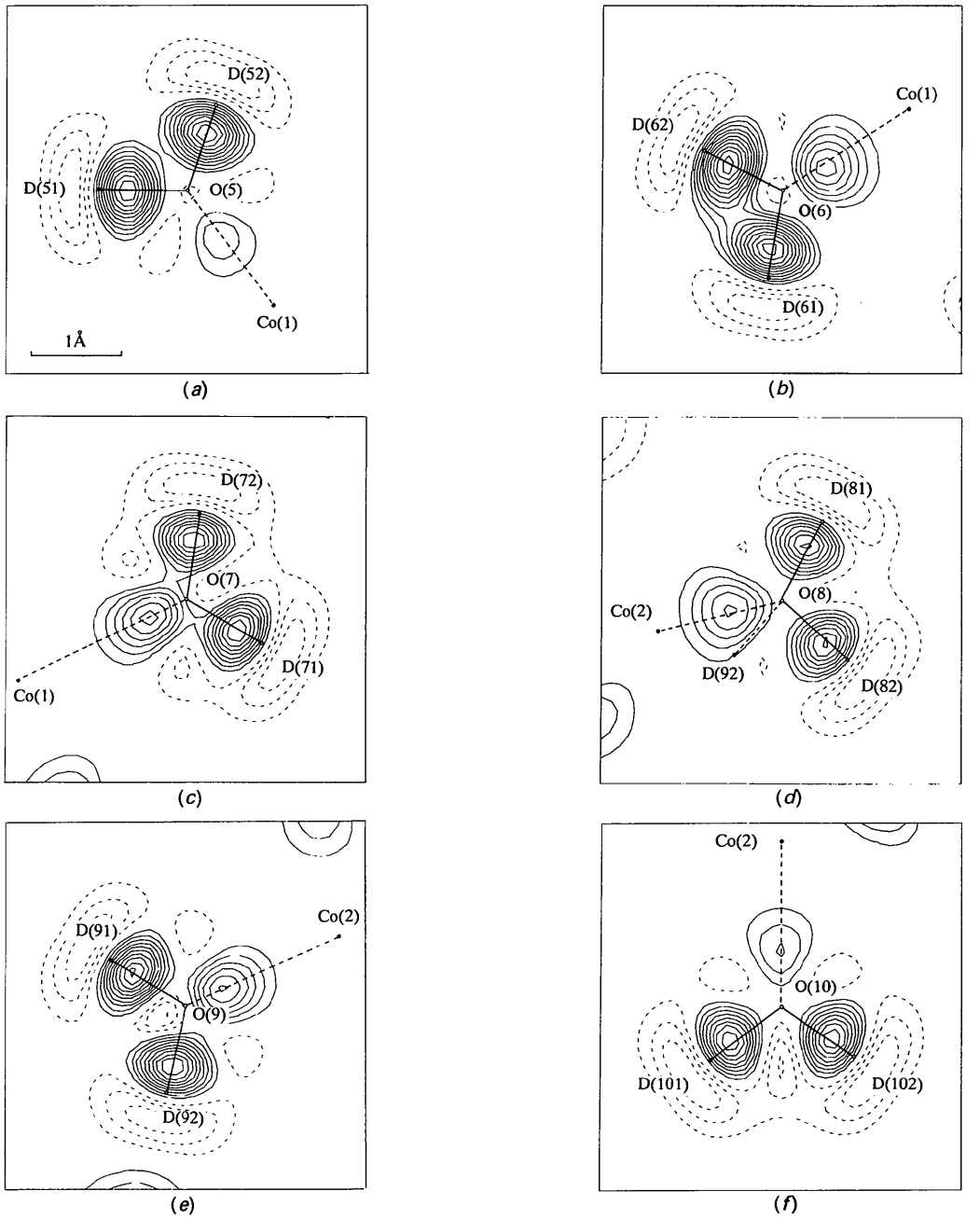

Fig. 5. Static deformation-model maps for the six independent water molecules [(*a*) to (*f*): O(5) to O(10)] calculated in the respective D—O—D planes. Only the deformation functions centred on the water molecules are displayed (see text). The scale given in (*a*) applies to all parts of the figure as well as to Fig. 6. For further explanation refer to the caption to Fig. 3.

McIntyre, 1993). Although care has been taken in the previous studies not to overinterpret the data, the accumulation of experimental evidence indicates that a trigonal coordination mode tends to deform the lone-pair density in such a way that only a single maximum is observed, whereas a tetrahedral coordination smears this maximum out in space and in some cases two somewhat separated maxima are observed. This tendency seems to be the more pronounced the stronger the polarizing power of the metal ion.

The superposition effect in the rather weak water–water hydrogen bond has also been examined. A comparison of the total and the individual deformation maps is given in Fig. 8. In this case, both maps are virtually identical and superposition effects are

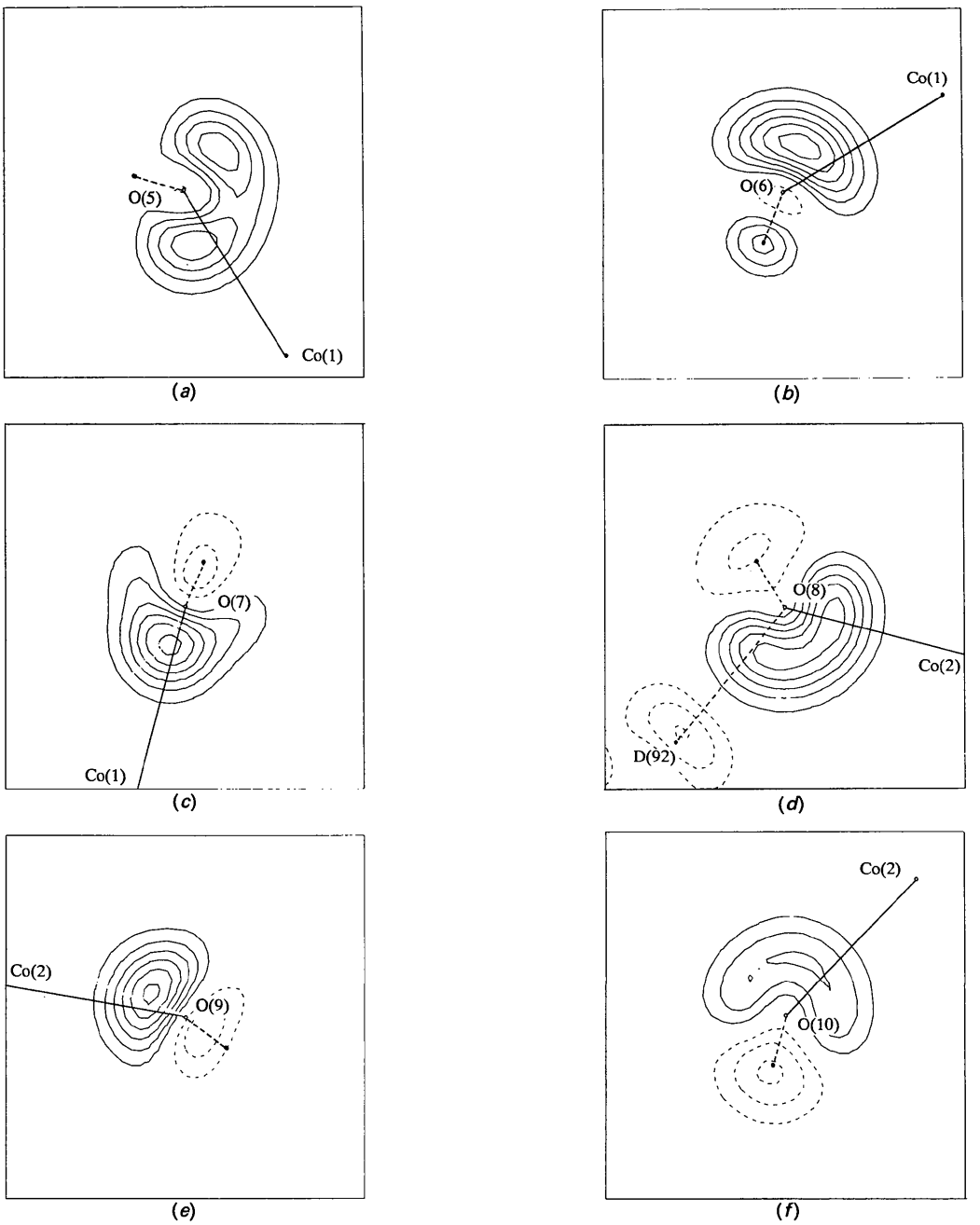

Fig. 6. Static deformation-model maps for the six independent water molecules [(*a*) to (*f*): O(5) to O(10)] calculated in the planes perpendicular to the respective D—O—D planes. For further explanation refer to the captions to Figs. 3 and 5.

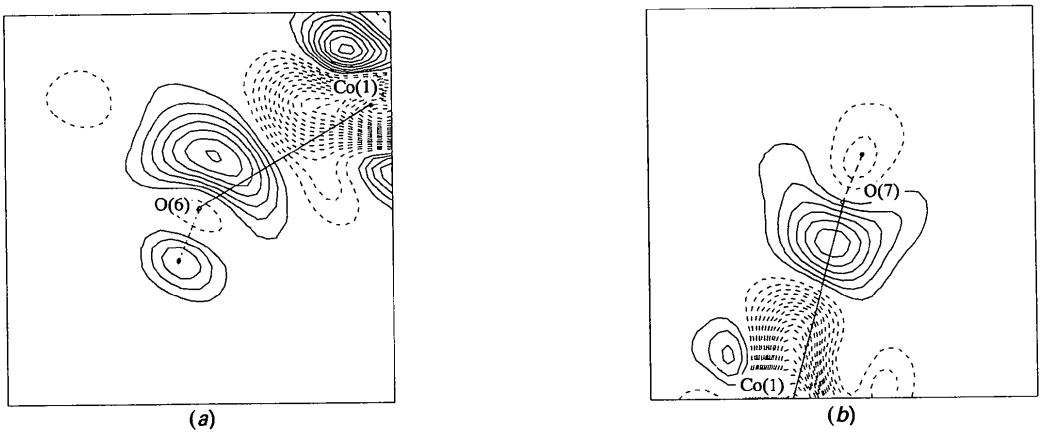

Fig. 7. Static deformation-model maps including the deformation functions of all atoms for (*a*) $D_2O(6)$ and (*b*) $D_2O(7)$ to be compared with Figs. 6(*b*) and 6(*c*). For further explanation refer to the captions to Figs. 3 and 5.

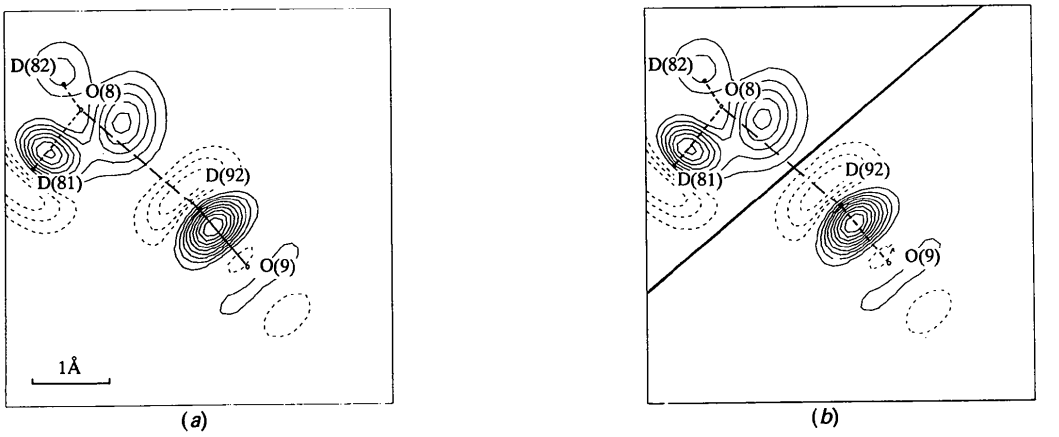

Fig. 8. Static deformation-model map in the plane of the O(9)—D(92)···O(8) hydrogen bond connecting two water molecules. (*a*) All atoms are included in the calculations. (*b*) A composite of two maps with only the deformation functions of $D_2O(9)$ (upper left) and $D_2O(8)$ (lower right). The heavy line shows the limit of the respective regions. For further explanation refer to the caption to Fig. 3.

negligible. This is in contrast to the corresponding situation in tetragonal $NiSO_4.6(H,D)_2O$ and can be attributed to the different hydrogen-bond lengths: 1.801 (2) Å for $NiSO_4.6H_2O$ (25 K) as opposed to 1.974 (2) Å in the present study. We conclude that a decomposition of the total density into individual contributions becomes essential when one deals with compounds containing strong and very strong hydrogen bonds – which have been the subject of most detailed electron density studies of intermolecular interactions in the past.

We would like to thank Professor J. O. Thomas and Drs K. Hermansson and H. Ptasiewicz-Bak for stimulating discussions, Mr H. Möller for preparing the Madelung potential plots, and Mr H. Karlsson for his skilful technical assistance with the X-ray data collection. The financial support provided by the Deutsche Forschungsgemeinschaft, the Swedish Natural Science Research Council and the Institut Laue–Langevin is gratefully acknowledged.

References

ABRAHAMS, S. C. & KEVE, E. T. (1971). *Acta Cryst.* A**27**, 157–165.
ALMLÖF, J., ROOS, B., WAHLGREN, U. & JOHANSEN, H. (1972). USIP Report 72-16. Univ. of Stockholm, Sweden.
ANGEL, R. J. & FINGER, L. W. (1988). *Acta Cryst.* C**44**, 1869–1873.
ANGERMUND, K., CLAUS, K. H., GODDARD, R. & KRÜGER, C. (1985). *Angew. Chem.* **97**, 241–252; *Angew. Chem. Int. Ed. Engl.* **24**, 237–247.
BECKER, P. & COPPENS, P. (1974). *Acta Cryst.* A**30**, 129–147, 148–153.
BECKER, P. & COPPENS, P. (1975). *Acta Cryst.* A**31**, 417–425.
CHIARI, G. & FERRARIS, G. (1982). *Acta Cryst.* B**38**, 2331–2341.
COPPENS, P. (1989). *J. Phys. Chem.* **93**, 7979–7984.
CROMER, D. T. & LIBERMAN, D. (1970). *J. Chem. Phys.* **53**, 1891–1898.
CROMER, D. T. & MANN, J. B. (1968). *Acta Cryst.* A**24**, 321–324.
DOYLE, P. A. & TURNER, P. S. (1968). *Acta Cryst.* A**24**, 390–399.
ELERMAN, Y. (1988). *Acta Cryst.* C**44**, 599–601.
FIGGIS, B. N., KUCHARSKI, E. S. & VRTIS, M. (1991). *Sagamore* X, *Collected Abstracts*, p. 35. Konstanz, Germany.
HALL, M. B. (1986). *Chem. Scr.* **26**, 395–408.
HAREL, M. & HIRSHFELD, F. L. (1975). *Chem. Scr.* **26**, 389–394.
HERMANSSON, K. (1984). *Acta Univ. Ups.* **744**.

HERMANSSON, K. (1985). *Acta Cryst.* B**41**, 161–169.
HERMANSSON, K., OLOVSSON, I. & LUNELL, S. (1984). *Theor. Chim. Acta*, **64**, 265–276.
HIRSHFELD, F. L. (1971). *Acta Cryst.* B**27**, 769–781.
HIRSHFELD, F. L. (1977). *Isr. J. Chem.* **16**, 226–229.
JOHNSON, C. K. (1976). *ORTEP*II. Report ORNL-5138. Oak Ridge National Laboratory, Tennessee, USA.
KELLERSOHN, T. (1992). *Acta Cryst.* C**48**, 776–779.
KELLERSOHN, T., DELAPLANE, R. G. & OLOVSSON, I. (1991). *Z. Naturforsch. Teil B*, **46**, 1635–1640.
LEHMANN, M. S. & LARSEN, F. K. (1974). *Acta Cryst.* A**30**, 580–584.
LUNDGREN, J. O. (1982). *Crystallographic Computer Programs.* Report UUIC-B13-04-05. Institute of Chemistry, Univ. of Uppsala, Sweden.
MCINTYRE, G. J., PTASIEWICZ-BAK, H. & OLOVSSON, I. (1990). *Acta Cryst.* B**46**, 27–39.
MASLEN, E. N., RIDOUT, S. C. & WATSON, K. J. (1988). *Acta Cryst.* B**44**, 96–101.
MASLEN, E. N. & SPADACCINI, N. (1989). *Acta Cryst.* B**45**, 45–52.
MASLEN, E. N., WATSON, K. J. & MOORE, F. H. (1988). *Acta Cryst.* B**44**, 102–107.
MENSCHING, L., VON NIESSEN, W., VALTAZANOS, P., RUEDENBERG, K. & SCHWARZ, W. H. E. (1989). *J. Am. Chem. Soc.* **111**, 6933–6941.
OLOVSSON, I. & JÖNSSON, P. G. (1976). *The Hydrogen Bond. Recent Developments in Theory and Experiments*, edited by P. SCHUSTER, G. ZUNDEL & C. SANDORFY, pp. 393–456. Amsterdam: North-Holland.
OLOVSSON, I., PTASIEWICZ-BAK, H. & MCINTYRE, G. J. (1993). *Z. Naturforsch. Teil A.* In the press.
PTASIEWICZ-BAK, H., MCINTYRE, G. J. & OLOVSSON, I. (1993). In preparation.
PTASIEWICZ-BAK, H., OLOVSSON, I. & MCINTYRE, G. J. (1993). *Acta Cryst.* B**49**, 192–201.
SAMSON, S., GOLDISH, E. & DICK, C. F. (1980). *J. Appl. Cryst.* **13**, 425–432.
SEARS, V. F. (1986). *Methods of Experimental Physics*, Vol. 23, *Neutron Scattering*, edited by K. SKÖLD & D. L. PRICE, pp. 521–550. New York: Academic Press.
THORNLEY, F. R. & NELMES, R. J. (1974). *Acta Cryst.* A**30**, 748–757.
WILKINSON, C., KHAMIS, H. W., STANSFIELD, R. F. D. & MCINTYRE, G. J. (1988). *J. Appl. Cryst.* **21**, 471–478.
ZALKIN, A., RUBEN, H. & TEMPLETON, D. H. (1962). *Acta Cryst.* **15**, 1219–1224.

Acta Cryst. (1993). B**49**, 192–201

Bonding Deformation and Superposition in the Electron Density of Tetragonal $NiSO_4.6H_2O$ at 25 K

BY H. PTASIEWICZ-BAK* AND I. OLOVSSON

Institute of Chemistry, University of Uppsala, Box 531, *S*-751 21 *Uppsala, Sweden*

G. J. MCINTYRE

Institut Laue–Langevin, BP 156, 38042 *Grenoble CEDEX* 9, *France*

(*Received* 12 *July* 1992; *accepted* 10 *September* 1992)

Abstract

The electron density in the title compound has been determined at 25 K by multipole refinement against single-crystal X-ray intensity data. Hydrogen positional and displacement parameters were fixed to values determined by refinement against single-crystal neutron data. The electron density based on the deformation functions of all atoms in the structure is compared with the individual densities calculated from the deformation functions of only nickel or the separate water molecules. In this way the effects of simple superposition of the individual densities have been studied. The individual deformation density around nickel is then in good qualitative agreement with that expected for an approximately octahedral $[Ni(H_2O)_6]^{2+}$ complex. The apparent decrease of the electron density in the lone-pair regions of the water oxygen atoms can be attributed to superposition of the oxygen density with the negative deformation density of nickel; the individual densities of the water molecules show clear polarization of the lone-pair densities according to the coordination of the water molecules. The individual densities of the water molecules are virtually identical with those earlier determined at room temperature. The densities around nickel show, however, clear differences: the heights of the outer negative lobes are increased, whereas those of the positive lobes are decreased as the temperature is raised from 25 K to room temperature. This is postulated to be due to a real change in the relative occupancy of the electronic energy levels. To the authors' knowledge this is the first time such an effect has been observed by diffraction methods. Crystal data: nickel sulfate hexahydrate, $NiSO_4.6H_2O$, $M_r = 262.86$, $P4_32_12$, $a = 6.7778$ (5), $c = 18.176$ (2) Å, $V = 834.98$ (2) Å^3, $Z = 4$, $T = 25$ K; λ(Mo $K\alpha$) = 0.71069 Å, μ =

* Permanent address: Institute of Nuclear Chemistry and Technology, Dorodna 16, 03-195 Warsaw, Poland.

0108-7681/93/020192-10$06.00